2D Electron Transport

Alon Shaaltiel, Oren Kereth & Gal Tuvia

April 3, 2022

Abstract

By subjecting a hetero-junction of GaAs/AlGaAs to an external magnetic field of varying strengths, at low temperature and under different voltage gates, the quantum and classical Hall effects were observed. Using the measurements, characteristics of the 2D electron gas (2DEG) were studied and compared to values from the literature. The sample was submerged in liquid helium under one atmosphere of pressure and under a vacuum to achieve low temperatures of 4.2K and 1.7K, respectively.

Part I
Background

In this experiment the Quantum Hall Effect (QHE) will be measured for a 2D electron gas formed at the hetero-junction of AlGaAs and GaAs.

1 Classical Hall Effect

At room temperature, when a small magnetic field ($B < 1T$) is applied perpendicularly to a current running from one side of a metal plate to the other, the classical Hall Effect can be observed and there is a measurable potential difference between the two remaining sides of the metal plate. This potential difference is normalized by the current, yielding the Hall resistance [6]

$$R_{xy} = \frac{V_H}{I} \tag{1}$$

where R_{xy} is the xy component of the resistance tensor (and also Hall resistance in this case)[9], V_H is the aforementioned potential difference and I is the current running through the metal plate. Using Drude's model one can formulate the relation between ρ_{xy}, the resistivity, and the applied magnetic field B to be[6]

$$\rho_{xy} = \frac{1}{ne}B \tag{2}$$

where n is the charge carrier density in the metal and e is charge of the electron. A similar expression can be written for the resistance R_{xy} due to the connection between the two. Note that this is valid only for small enough magnetic fields, depending on the temperature.

2 Quantum Hall Effect

QHE can be observed at low temperatures and for strong enough magnetic fields $(B > 1T)$ for the 2D electron gas. As the name suggests, this phenomena is explained using quantum mechanics. The 2D electron gas is formed on the layer between two different semiconductors whose Fermi level is different. Due to the difference in Fermi levels, near the hetero-junction the band structure of both semiconductors is altered, effectively creating a finite potential well for the electrons occupying the boundary layer. As a result, these electrons are confined in their movement and are practically two dimensional[9]. Having a 2D electron gas is essential for the measurement of QHE as it allows the creation of discrete energy states with large degeneracy using a magnetic field known as Landau Levels[9]. Measurement of ρ_{xy}, ρ_{xx} vs B yields the following graphs:

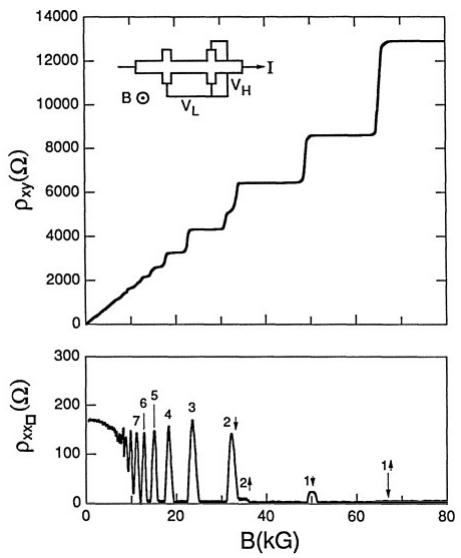

Figure 1: QHE - ρ, the resistivity in different directions vs B, the applied magnetic field[2]

Note that for small magnetic fields ρ_{xy} changes linearly with B, fitting the classical Hall Effect, which is valid for small magnetic fields as mentioned. However, for larger magnetic fields plateaus of constant resistance at very specific values can be seen. Moreover, corresponding to these plateaus on the ρ_{xx} graph there are also plateaus of 0 resistance (which are in fact infinite resistance such that no current can flow). These graphs are analyzed more thoroughly later on. Using the measurement of QHE, valuable information regarding the electron gas can be extracted, as is done in the following sections in this report.

Part II

Experimental Setup

As was previously mentioned, in this experiment we study the 2D electron gas in the hetero-junction between AlGaAs and GaAs. In order to do so, a sample of the aforementioned hetero-junction is lowered into liquid helium with various probes, a temperature sensor and a capacitor. The Dewar which holds the liquid helium also cooled a superconducting coil which acts as a high-power magnet when current is passed through it. The probes are drawn in Figure 2, probes 5 and 15 allow a current to be passed through the sample, probe 5 is connected to the source of a lock-in amplifier and probe 15 is grounded. The same source is also connected in series to a $1\,\mathrm{M}\Omega$ resistor, which is then grounded. As both probe 15 and the connection to the resistor are grounded they are connected through the "ground" (a large metal board in our case). The resistance on the source is $1\,\mathrm{M}\Omega + R_{2DEG}(T) = R_{tot}$, as $R_{2DEG}(T) \approx 1\,\mathrm{k}\Omega$, we can assume the resistance, and thus current, are not dependent on the sample's temperature. This is done to reduce fluctuations in later resistance measurements.

Probes 6 and 11 were used to measure the voltage across the 2D electron gas with a lock-in amplifier, the lock-in amplifier then measures the resistance across using the current that is fed from the source, which is connected to probes 5 and 15. In a similar fashion, probes 6 and 3 were used to measure the resistance in perpendicular to the current's direction.

Probe 1 is used to induce a voltage on the gold plate above the 2D electron gas, the plate is grounded and like the resistor is thus connected to probe 15. This allows it to carry a voltage potential relative to the electron gas and create an electric field, which changes the available states in the gas, thus changing the carrier density.

Both lock-in resistance readings, the temperature near the sample and the magnetic field in the superconducting coil were fed into and operated by a LabView application at the lab. The application could command the parts to change one aspect (i.e. the gate voltage, or current in the coil) at a given rate and measure all quantities during the process. The working range was -0.5 Volt to 0.5 Volt for the gate voltage and 0 to 5.5 Tesla for the superconducting coil. Do note that the temperature sensor's readings change under a magnetic field.

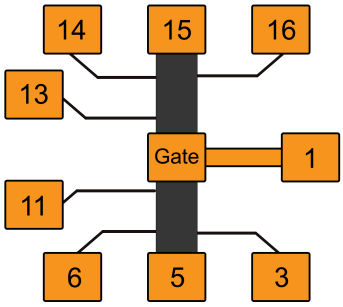

Figure 2: A representation of the hetero-junction sample, its probes and the capacitor. The 2D electron gas is colored in dark gray, and the probes and gold plate which serves as a capacitor, in orange. The capacitor is positioned above the 2D electron gas.

In the first set of measurements, the resistance R_{xx} was measured versus the temperature T, changing from room temperature to $4.2K$ due to the boiling helium inside the Dewar. After the 2DEG stabilized on $4.2K$ several measurements were made. One set of measurements was done by setting the voltage gate to a constant value and then measuring the resistances R_{xx}, R_{xy} while changing the magnetic field from $0T$ to $5.5T$. The voltage gate value was either $0, -0.5$ or 0.5 volts. Another set of measurements was made by setting the magnetic field to a constant value of either $0.5T$ or $5T$ and measuring the resistance while changing the voltage gate from $-0.5V$ to $0.5V$. After performing these measurements the temperature of the sample was further lowered by creating a vacuum using a pump (see Figure 3)

Figure 3: Experimental Setup - in the middle: the Dewar which holds the helium. Right above it the sample was inserted on a rod through the metal pipe. To the right of the helium Dewar is the pump with which the vacuum was created.

After lowering the temperature to the vicinity of $1.7K$ (as there were some fluctuations) the same measurements detailed above were done again.

Part III
Measurements

Sheet Resistance vs Temperature

As mentioned above, at the beginning of the experiment the sample was cooled from 300K to 4.2K with $B = 0$. During this cooling process, its resistance R_{xx} was measured and plotted versus the temperature. Because the measured resistance is the total resistance of two resistors connected in parallel - the first being the 2D electron gas and the second being AlGaAs, effects regarding the resistance as a function of temperature for both resistors must be taken into account. For the 2D electron gas the resistance can be expressed as

$$R_{2DEG}(T) = a_0 + a_1 T^3 + a_2 T^5 \tag{3}$$

where a_0, a_1, a_2 are coefficients, T is the temperature and R_{2DEG} is the resistance of the 2D electron gas. Note that for $T \to 0$ the resistance is not 0 due to impurities in the material and that for higher temperatures the contributions of

T^3, T^5 are due to phonons and thermal excitation occurring in the electron gas[6], leading to a higher resistance. The behavior of the resistance as a function of the temperature for the semiconductor is different than that of the 2DEG as thermal exications in the semiconductor actually reduce the resistance by allowing the electrons to move from the valence shell to the conductance shell, thus contributing to the conduction of the material. Therefore the resistance is

$$R_{SC}(T) = b_0 + b_1 e^{\frac{2E_g}{k_B T}} \tag{4}$$

where b_0, b_1, E_g are coefficients and R_{SC} is the resistance of the semiconductor. E_g is the energy gap between the valence shell and the conductance shell and it can be seen that for higher temperatures the resistance becomes lower as opposed to the electron gas whose resistance becomes higher. Because the two resistors are parallel to each other the total resistance which is the one measured is[4]

$$\frac{1}{R} = \frac{1}{R_{2DEG}} + \frac{1}{R_{SC}} \tag{5}$$

Notice that for low temperatures $R_{SC} \to \infty$ and so the semiconductor does not contribute to the total resistance and for high temperatures the opposite occurs. Therefore, by fitting the resistance in low temperatures to 3 and the resistance in high temperatures to 4 all the coefficients $a_0, a_1, a_2, b_0, b_1, E_g$ can be extracted. . By measuring the resistance for each temperature and by fitting the two temperature regions to the corresponding functions the following graphs and parameters have been extracted:

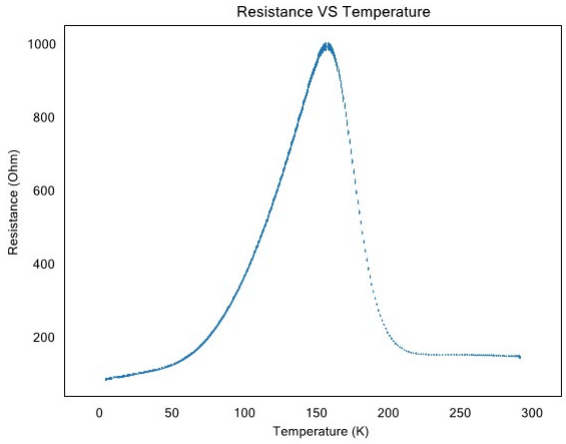

Figure 4: Resistance VS Temperature - The entire range

It can be seen that for low temperatures the resistance acts like some polynomial and that for high temperatures it acts like an exponential function, matching the theory above. By fitting each region the following was extracted:

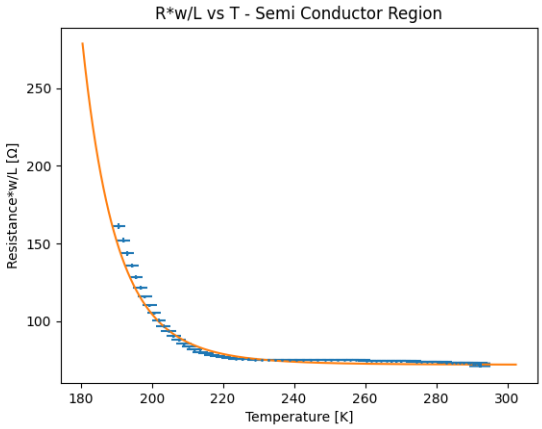

Figure 5: Resistivity VS Temperature - High Temperature region

where w and L are the width and length of the sample correspondingly. The corresponding parameters and statistical values.

Parameter	Value	Error	Relative Error
$b_0[\Omega]$	72.010	0.081	0.11%
$b_1[\Omega]$	1.26×10^{-6}	8.1×10^{-7}	64%
$E_g/k_B[K]$	1707	67	3.9%
χ^2_{red}	1.3	———	
P_{value}	0.0010	———	

Table 1: Resistivity VS Temperature Fit Parameters of the high temperature region

For the low temperature region:

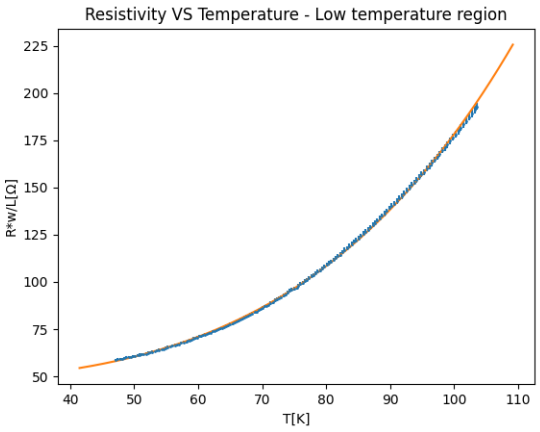

Figure 6: Resistivity VS Temperature - Low Temperature region

with the corresponding parameters and statistical values

Parameter	Value	Error	Relative Error
$a_0[\Omega]$	46.90	0.13	0.28%
$a_1[\Omega/K^3]$	1.0010×10^{-4}	9.2×10^{-7}	0.92%
$a_2[\Omega/K^5]$	3.134×10^{-9}	9.2×10^{-11}	2.9%
χ^2_{red}	0.28	————	
P_{value}	1.0	————	

Table 2: Resistance VS Temperature Fit Parameters of the low temperature region

For the high temperature region fit, the statistical values suggest an under-estimation of error as the theory describes the behavior of the resistance in that region properly, with the resistance changing exponentially with $\frac{1}{T}$. The low temperature fit is adequate, as can also be seen from the statistical values and from the fit itself. Overall, both fits are good and the theory describes the physical phenomena well. Using the fit parameters from both fits and equations 3,4 and 5 a graph consisting of both the original measurements and the final fit for the entire region was plotted (see Figure 7)

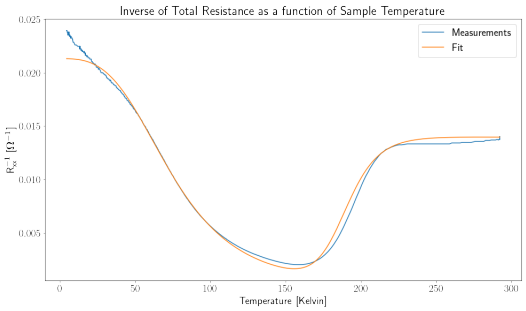

Figure 7: $\frac{1}{R_{xx}}$ VS T for the entire region of measurements. In orange- equation 5 with the fit parameters of both fits substituted in 3 and 4. In blue- the measurements.

It can be seen that the final fitting function using the fit parameters from the previous fits describes the physical phenomena adequately. Further analysis can be found in the Discussion.

Low Field Regime

As explained in the experimental setup, in this part of the experiment the resistance of the 2DEG was measured for different gate voltages and different constant temperatures. In low magnetic fields R_{xy}, R_{xx} exhibits a behavior described by the classical Hall Effect and the Drude model [6]. By fitting a linear function

$$R_{xy} = a_0 + a_1 B \tag{6}$$

where according to 2 a_0 should be consistent with 0 and $a_1 = \frac{1}{ne}$. Using the linear fit, the charge carrier density of the 2DEG can be extracted from a_1 by

$$n = \frac{1}{a_1 e} \tag{7}$$

By measuring R_{xx}, which according to Drude model, is constant, one can extract the mean free time between electrons, τ_t, through the relation between the two:

$$R_{xx} = \frac{m^*}{ne^2\tau_t} \tag{8}$$

where m^* is the effective mass[6] of the 2DEG. Several fits were made; 3 fits for each temperature (1.7K and 4.2K),

each fit with a different gate voltage V_G. By changing the gate voltage the charge carrier density of the 2DEG changes, thus yielding different linear graphs with varying slopes. Using the mean free time, τ_t, the mobility, μ ,of the 2DEG can be extracted [6]

$$\mu = \frac{e\tau_t}{m^*} \tag{9}$$

By fitting linear function to the 3 different gate voltages for $T = 4.2K$ the following was extracted (see Figure 8, only $V_g = -0.5$ is shown, the rest are similar.)

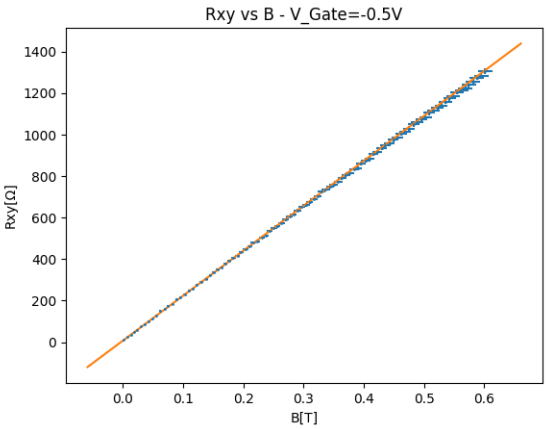

Figure 8: Classical Hall Effect - R_{xy} VS B at $T = 4.2K$ for $V_g = -0.5\,V$

with the corresponding n,τ_t,μ and fit parameters (see Tables 3 and 4)

$V_G[V]$	$n[10^{15}1/\mathrm{m}^2]$	χ^2_{red}	P_{value}
0.5	$6.917 \pm 8.9 \times 10^{-2}(1.3\%)$	30	0.0
0	$4.677 \pm 1.5 \times 10^{-2}(0.32\%)$	1.5	0.0010
-0.5	$2.8803 \pm 5.0 \times 10^{-3}(0.17\%)$	0.52	1.0

Table 3: Extracted values from the linear fits for R_{xy} VS B at $T = 4.2K$

$V_G[V]$	$\mu[\mathrm{C}*\mathrm{sec}/\mathrm{kg}]$	$\tau_t[10^{-12}sec]$
0.5	$23.54 \pm 0.39(1.7\%)$	$8.97 \pm 1.5 \times 10^{-1}(1.7\%)$
0	$17.51 \pm 0.18(1.0\%)$	$6.674 \pm 7.0 \times 10^{-2}(1.0\%)$
-0.5	$8.961 \pm 0.092(1.0\%)$	$3.413 \pm 3.5 \times 10^{-2}(1.0\%)$

Table 4: Additional extracted values from the linear fits for R_{xy} VS B at $T = 4.2K$

By fitting linear function to the 3 different gate voltages for $T = 1.7K$ the following was extracted (see Figure 9, only $V_g = 0.5V$ is shown while the rest are similar.)

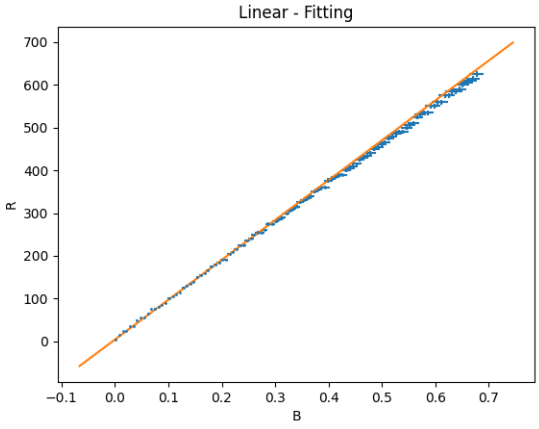

Figure 9: Classical Hall Effect - R_{xy} VS B at $T = 1.7K$ for $V_G = 0.5V$

with the corresponding n,τ_t,μ and fit parameters (see Tables 5 and)

$V_G[V]$	$n[10^{15}1/\mathrm{m}^2]$	χ^2_{red}	P_{value}
0.5	$6.693 \pm 4.0 \times 10^{-2}(0.60\%)$	6.8	0.0
0	$4.731 \pm 1.6 \times 10^{-2}(0.34\%)$	2.0	0.0
-0.5	$2.8173 \pm 4.9 \times 10^{-3}(0.17\%)$	0.59	1.0

Table 5: Fit Parameters from the linear fits for R_{xy} VS B at $T = 1.7K$

$V_G[V]$	$\tau_t[10^{-12}sec]$	$\mu[\mathrm{C\cdot sec/kg}]$
0.5	$10.142 \pm 1.2 \times 10^{-2}(0.12\%)$	$26.623 \pm 0.032(0.12\%)$
0	$6.961 \pm 7.3 \times 10^{-2}(1.0\%)$	$18.27 \pm 0.19(1.0\%)$
-0.5	$3.338 \pm 3.4 \times 10^{-2}(1.0\%)$	$8.76 \pm 0.10(1.1\%)$

Table 6: Extracted values from the linear fits for R_{xy} VS B at $T = 1.7K$

Overall, for all the measurements at both temperatures and for all the different values of the voltage gate it can be seen that the fits are adequate and a linear fit indeed describes the phenomena (despite the somewhat inadequate statistical values for some of them). In addition, all values extracted from the fit parameters seem to be in line with expected values. The charge carrier density came out lower than that of other materials, fitting the information we have about the 2DEG and what we were told in the lab. Moreover, τ_t is of the appropriate scale compared to other materials[8]. Another thing to note is that when lowering the temperature from $4.2K$ to $1.7K$ it can be seen that τ_t, on average, becomes longer. Meaning there are less collisions in a given period of time. Further analysis can be found in the Discussion.

As was mentioned in the 'Experimental Setup' section, measurements under a constant magnetic field and a changing gate voltage were also made. The relevant measurement to this section is that under a magnetic field of $0.5\,Tesla$. The capacitance of the gate is $C = \frac{Q}{V_g} = \frac{Ane}{V_g} = \frac{\varepsilon_0\varepsilon_r A}{d}$ where the last relation is a known capacitor property. By dividing both sides by A we get $\frac{ne}{V_g} = \frac{\varepsilon_0\varepsilon_r}{d}$, substituting ne by $\frac{1}{R_{xy}}$, from the classical Hall effect, and lastly, multiplying by V_g we get the relation:

$$\frac{1}{R_{xy}}(V_g) = \frac{\varepsilon_0\varepsilon_r}{d}V_g \tag{10}$$

where $\varepsilon_0\varepsilon_r$ is the permittivity of the sample (taken to be the permittivity of $GaAs$), d is the distance of the gate from the sample, V_g is the gate voltage and R_{xy} is the resistance perpendicular to current flow.

A linear fit of the form:

$$y = a_0 + a_1 x$$

was made, where y is $\frac{1}{R_{xy}}$, x is V_g, a_1 has a theoretical value of $\frac{\varepsilon_0\varepsilon_r}{d}$ and a_0 has a theoretical value of 0 (see Figure 10).

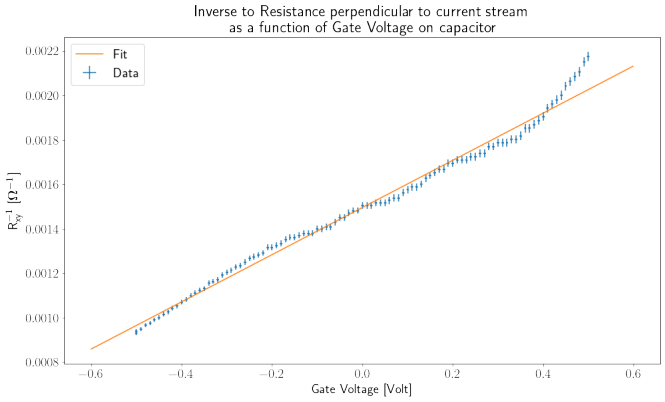

Figure 10: A linear fit to R_{xy}^{-1} as a function of V_g under a magnetic field of $0.5\,Tesla$

The fit parameters for the fit are presented in Table 7.

Parameter	Value	Error	Relative Error
$a_0\,[\Omega^{-1}]$	1.4952×10^{-3}	3.2×10^{-6}	0.21%
$a_1\,[\Omega^{-1}/\mathrm{Volt}]$	1.061×10^{-3}	1.0×10^{-5}	0.94%
χ^2_{red}	4.3	———	
P_{value}	4.4×10^{-42}	———	

Table 7: Fit parameters for the fit in Figure 10

The statistical values are out of their corresponding desired ranges, yet Figure 10 shows that the a linear fit describes the phenomena adequately with some needed tweaks corresponding to a higher order polynomial or an oscillating function. Using the permittivity of $GaAs$ found in the literature [3] and Eq. 10 the distance of the gate from the 2D electron gas was found to be $d = 1.097{\times}10^{-7}{\pm}1.1{\times}10^{-9}\,[m]$.

High Field Regime

Continuing the last section, both R_{xy} and R_{xx} were measured under a high magnetic field, up to 5.5 Tesla, while changing the gate voltage on the 2D electron gas.

R_{xy}'s behavior is described by the Integer Quantum Hall Effect and is characterized by plateaus along a linear line. The resistance at each plateau is an integer multiple of $R_K = \frac{h}{e^2} = 25800\,\Omega$[9] , and because of spin degeneracy,

unless the spin states are separated, only even integers are seen.

R_{xx}'s behavior is described by Shubnikov–de Haas oscillations, which is characterized by big peaks corresponding to Landau Levels in R_{xy} and 0 resistances corresponding to the plateaus.

If one looks at the behavior of R_{xx} vs. $\frac{1}{B}$ all peaks should come at a regular interval with decreasing amplitude. By calculating that regular interval the carrier density can be found:

$$n = 2 \cdot \frac{e}{h\Delta(B^{-1})} \tag{11}$$

where h is Planck's constant, e is the elementary charge , $\Delta(B^{-1})$ is the regular interval between peaks and the 2 is due to the degeneracy caused by spin[9].

The charge carrier density was calculated for all gate voltages and both temperatures. The peaks for each configuration were found using python and have a relative error of about 1%.

Figure 11 shows the identified peaks for the measurements under a gate voltage of $V_g = 0.5\,V$ and a temperature of $T = 1.7\,K$.

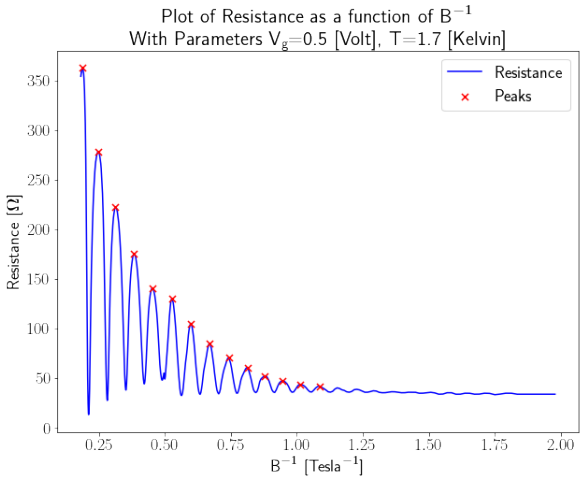

Figure 11: Plot of R_{xx} as a function of $\frac{1}{B}$ for $V_g = 0.5\,V$ and $T = 1.7\,K$ with peaks highlighted by red x-es

As can be seen, the peaks are equidistant from each other with an average distance of $\Delta(B^{-1}) = 0.06988 \pm 0.00027\,(0.38\%\ \text{Tesla}^{-1})$.

The extracted carrier densities are presented in Table 8.

$V_g\,[V]$	$T\,[K]$	$n\,[10^{15}/\text{m}^2]$
0.5	4.2	$6.921 \pm 0.026\,(0.38\%)$
0		$4.6875 \pm 0.0087\,(0.19\%)$
−0.5		$2.934 \pm 0.033\,(1.1\%)$
0.5	1.7	$6.994 \pm 0.030\,(0.43\%)$
0		$5.012 \pm 0.080\,(1.6\%)$
−0.5		$3.235 \pm 0.085\,(2.6\%)$

Table 8: Extracted carrier densities for the various configurations

These figures are in great agreement with those extracted using the classic Hall effect. Notice that both final calculated densities have a higher uncertainty, that is because one of the peaks was a peak separated from others by the Zeeman effect corresponding to an odd Landau Level (3 and 5).

Note how the amplitude of the peaks is lessened over smaller magnetic fields (i.e bigger $\frac{1}{B}$s), the formula for the envelope function of the SdH oscillations is [1]:

$$\Delta R(T, B^{-1}) = 4R_0 \frac{2\pi^2 \mathrm{m}^* \mathrm{k_B T \cdot B^{-1}}/\hbar \mathrm{e}}{\sinh(2\pi^2 \mathrm{m}^* \mathrm{k_B T \cdot B^{-1}}/\hbar \mathrm{e})} e^{-\frac{\pi m^*}{e\tau_q} B^{-1}} \tag{12}$$

where ΔR is the peak difference in resistance, m^* is the electron's effective mass, k_B is Boltzmann's constant, T is the 2DEG's temperature and τ_q is the scattering time corresponding to the dephasing of the Landau state [9]. Before fitting the data to the function written above the effective mass, m^* of the 2DEG has to be extracted. The resistance R_{xx} was measured for two different temperatures - $T_1 = 1.7K$ and $T_2 = 4.2K$. By dividing the amplitude of each peak measured at T_2 by its corresponding peak at T_1 one can derive

$$y = \frac{T_2}{T_1} \frac{\sinh(2\pi^2 \mathrm{m}^* \mathrm{k_B T_1 B^{-1}}/\hbar \mathrm{e})}{\sinh(2\pi^2 \mathrm{m}^* \mathrm{k_B T_2 B^{-1}}/\hbar \mathrm{e})} e^{-\frac{\pi m^*}{e}(\frac{1}{\tau_q(T_2)} - \frac{1}{\tau_q(T_1)})B^{-1}} \tag{13}$$

where the ratio was defined as $y = \frac{\Delta R(T_2, B^{-1})}{\Delta R(T_1, B^{-1})}$ and it was assumed that the scattering time τ_q is temperature dependent. Therefore, by fitting

$$y(x) = a_0 \frac{sinh(\frac{T_1}{T_2} a_1 x)}{sinh(a_1 x)} e^{-a_2 x} \tag{14}$$

where $x = \frac{1}{B}$ and the fact that both sinh-s are the same apart for the temperature was used, using the fit parameter a_1, the effective mass can be found $m^* = \frac{a_1 \cdot \hbar e}{2\pi^2 k_B \cdot 1.7}$ (see Figure 12)

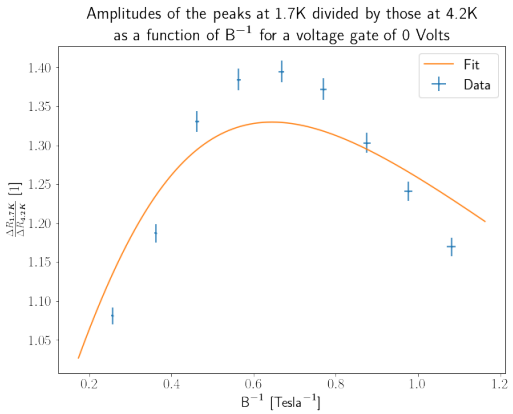

Figure 12: y VS $\frac{1}{B}$ for $V_g = 0$

The corresponding fit parameters and extracted effective mass are (see Table...)

Parameter	Value	Error	Relative Error
$a_0\,[1]$	1.83	0.98	54%
$a_1\,[Tesla]$	1.9	2.1	110%
$a_2\,[Tesla]$	2.4	3.5	150%
$m^*\,[10^{-32}kg]$	6.8	7.7	110%
χ^2_{red}	22	———	
P_{value}	1.1×10^{-25}	———	

Table 9: Fit parameters and extract effective mass from the y VS $\frac{1}{B}$ at $V_g = 0$ fit

After finding the effective mass from one of these fits, τ_q can now be extracted from the data using a fit of the form

$$\Delta R(T,x) = a_0 \frac{a_1 x}{\sinh(a_1 x)} e^{-a_2 x} \tag{15}$$

was made to the peaks of each configuration after the average resistance at a very low field was subtracted. Using the fitted parameters the quantities τ_q can be calculated

$$\tau_q = \frac{\pi m^*}{e a_2} \tag{16}$$

Figure 13 shows one of the fits, which represents all others quite well in goodness of fit.

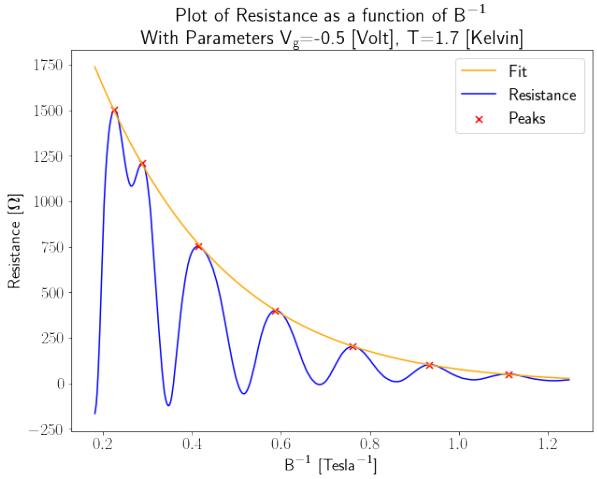

Figure 13: Plot of R_{xx} as a function of B^{-1} with resistance peaks represented as red x-es. A fit to the envelope function was made and is represented in orange

The extracted τ_q values and their comparison with τ_t are shown in Table 10

$V_g\,[V]$	$T\,[K]$	$\tau_q[10^{-12}s]$	$\frac{\tau_t}{\tau_q}$	χ^2_{red}	P_{value}
0.5	4.2	$1.19 \pm 0.20(17\%)$	7.7	1.6	0.099
0		$0.545 \pm 0.026(4.8\%)$	12	1.0	0.14
−0.5		$1.04 \pm 0.17(16\%)$	3.3	0.61	0.68
0.5	1.7	$0.3684 \pm 0.0094(2.6\%)$	28	0.68	0.61
0		$0.448 \pm 0.016(3.6\%)$	16	0.35	0.98
−0.5		$0.4156 \pm 0.0036(0.87\%)$	8.3	0.40	0.94

Table 10: τ_q extracted from SDH oscillations fit of R_{xx} VS $\frac{1}{B}$

On average τ_q is smaller than τ_t in about one order of magnitude. Further analysis is presented in the Discussion.

3 Quantum Hall Regime

In this part of the experiment the plateaus in the R_{xy} graph (see Figure 1) were extracted and their corresponding resistance value was used in order to extract the filling factor ν

using the equation [9]

$$R_{xy} = \frac{1}{\nu}\frac{h}{e^2} \tag{17}$$

where h is the Planck constant. First of all the plateaus in each set of measurements were identified (see Figures 14 and 15, other configurations are similar.)

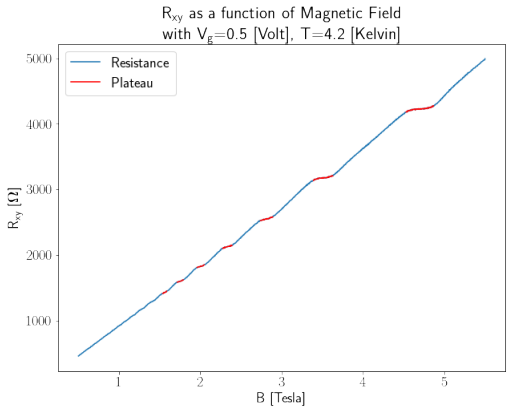

Figure 14: R_{xy}VS B with $T = 4.2K$ and $V_G = 0.5V$. The plateaus are labeled in red.

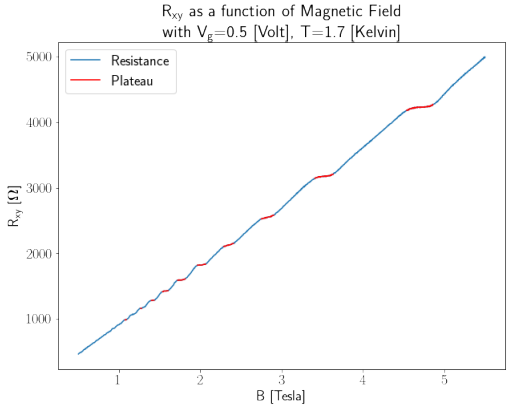

Figure 15: R_{xy}VS B with $T = 1.7K$ and $V_G = 0.5V$. The plateaus are labeled in red.

The filling factors extracted for each graph can be seen in Table 11

Filling Factors Table		
$T[K]$	$V_G[V]$	First Extracted ν-s
4.2	-0.5	$8.10, 6.08, 4.08, 2.09$
	0	$10.12, 8.10, 6.07, 4.06$
	0.5	$12.13, 10.14, 8.13, 6.11$
1.7	-0.5	$6.08, 4.07, 3.05, 2.06$
	0	$8.09, 6.07, 5.08, 4.06$
	0.5	$12.13, 10.14, 8.13, 6.11$

Table 11: Filling Factor ν for each temperature and voltage gate

For all graphs the filling factor ν came out quite close to an integer value. For $T = 4.2K$, ν is even, as was expected due to spin degeneracy and as was explained in previous sections. However, for $T = 1.7K$, ν took on odd values as well. This is due to the spin degeneracy being lifted as a result of the spin interaction with the magnetic field- Zeeman effect [5]. Further analysis can be found in the discussion. After extracting the filling factors both $R_{xx}$and R_{xy} were plotted VS the voltage gate V_g at a constant magnetic field of $B = 5T$ yielding (see Figures 16 and 17)

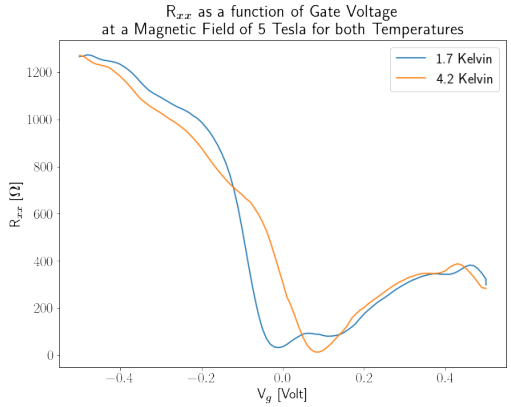

Figure 16: R_{xx} vs V_g at a magnetic field of 5 Tesla for both temperatures. Orange- 4.2K and blue- 1.7K

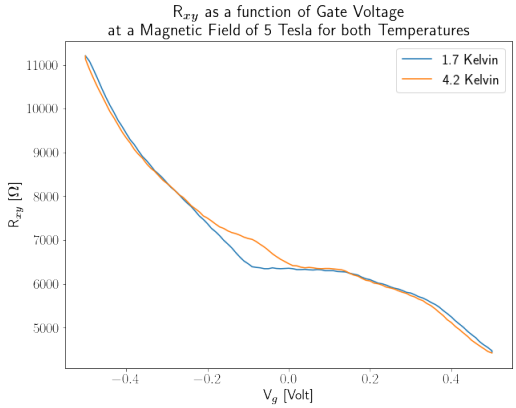

Figure 17: R_{xy} vs V_g at a magnetic field of 5 Tesla for both temperatures. Orange- 4.2K and blue- 1.7K

For both temperatures the change in voltage gate led to a change in the highest Landau level being occupied. This can be identified in R_{xy} by noticing the plateau at around $V_g = -0.1V$ for $T = 1.7K$ or around $V_g = 0.1V$ for $T = 4.2K$. A part of SDH oscillations can also be spotted in R_{xx}—at corresponding values of the voltage gate a sudden drop in resistance can be noticed. Further analysis at the Discussion.

Part IV

Discussion

Sheet Resistance VS Temperature

In this part of the experiment the sheet resistance R_{xx} was fitted according to the model of two resistors connected in parallel, one is the 2DEG and the other is a semiconductor. Each of these resistors behaves differently under temperature change and become dominant in different temperature regions. We used this information in order to perform 2 fits- one in high temperatures and the other in low temperatures. Using the fit parameters extracted from these two fits another plot was made for the entire region using 5 yielding Figure 7. As was mentioned previously it can be seen that the model describes the phenomena adequately. It can be seen, however, that in the middle of the graph (around $T = 160K$) there is somewhat of an inconsistency between the function and the original measurements. The functions seems somewhat "delayed" compared with the measurements. A source for this problem could be that the two previously mentioned fits, each in its respective regions, were still effected by the existence of the other region; i.e. in low temperatures, towards temperatures of about $T \sim 100K$, the semiconductor would still have an effect on the fit that was not taken into account. The same thing can be said about higher temperatures of about $T \sim 200K$ where the 2DEG affects the fit for the semiconductor. This explanation is also validated by the two fits 5 and 6 where towards the middle range temperature (between $100 - 200K$) the measurements in both fits seem to deviate from the fitted function, also leading to the somewhat inadequate statistical values extracted from these fits. Regardless, the model we used in this part of the experiment seems to work well in describing the change of the resistance with temperature.

Low Field Regime

Using the classical Hall Effect in equation 2, Drude model and by measuring R_{xx}, R_{xy} in low magnetic fields, the charge carrier density, n, the free time between collision, τ_t and the mobility of the charge carrier, μ, were all extracted at different temperatures and voltage gates. In all graphs it can be seen that the linear fit describes the dependency of the resistance in the magnetic field for low fields quite well. The good fit with lacking statistical parameters suggest an under-estimation of uncertainty. Regardless, the fits were adequate and the extracted values are in line with what we expected. The charge carrier density changes with the voltage gate in an expected manner- higher voltage gate leads to higher charge carrier density (and not the opposite - since the electrons have negative charge).
In the second part of the Low Field Regime section we tried to extract the distance of the gate from the sample. The statistical parameters were outside their desired ranges, as the fit is overall very good, this is likely because of the very small uncertainty in the measurements. The extracted distance is of the a scale likely to be used in this experiment. As we do not know the real distance, no comparison can be made.

High Field Regime

In this section of the experiment we analyzed the behavior of the 2D electron gas under a high magnetic field ($B > 0.5 Tesla$). We observed Landau Levels, the integer quantum Hall effect and Shubnikov–de Haas oscillations. We started by extracting the carrier densities for different temperatures and gate voltages. These can be compared to the carrier densities extracted using the classical Hall effect and are at a distance of 1% to 10% at worst. Do also note that the carrier density is directly correlated with gate voltage, the higher the gate voltage the higher the carrier density, just as it was in the low field regime. This is in great agreement with the theory. Afterwards, using the peaks of the oscillations and the known envelope function we attempted to extract the effective mass and quantum lifetime. The effective mass of the 2DEG came out close to the theoretical value however, it has a large uncertainty. Using the effective mass and by performing several fits, the quantum lifetime was extracted for different temperatures and voltage gates. The fits from which τ_q was extracted were quite good, yielding good statistical values. Comparing the extracted values of τ_q to those in the literature [7] yielded good results as they are of the same magnitude. However, it is clear there is some difference between the values, this can also be demonstrated in the ratio τ_t/τ_q which came out smaller compared to [7]. An explanation for these inconsistencies could be that the temperature was not constant throughout the measurements. When the measurements for $T = 1.7K$ were made, T was not always constant, as a matter of fact it got lower throughout our measurements in a way we could not control. The changing temperature has a great effect on the fit from which the effective mass was extracted as it was assumed that the two temperatures were constant. If the temperatures changed between peaks, a fit that assumes otherwise will not be as good. A possible explanation for the difference in goodness of fit between the effective mass and the quantum lifetime portion is the general behavior of the fitting functions. The function $\frac{ax}{sinh(ax)}$ decays, a larger a leads to a faster decay rate. Multiplying this function by a decaying exponent yields $\frac{ax}{sinh(ax)}e^{-bx}$ (which is the function fitted to find τ_q). Since these are two decaying functions, both of which decay exponentially, over a short enough sample, it can be quite well approximated as Ae^{-Cx} where C takes into consideration both decay rates. This practically means that the first decaying function is quite redundant and that it has little effect on how well the fit could be (as a matter of fact we tried fitting the peaks of R_{xx} to a decaying exponent which led to just as good fits). As a result, the small temperature changes would have almost no effect on the quality of the fit, but they will alter the decay rates, that are directly connected to τ_q. Conversely, in order to find m^* a fit of the form $\frac{sinh(ax)}{sinh(bx)}e^{-cx}$ was made. Unlike the first case, these are not two decaying functions multiplied by each other and the part of $\frac{sinh(ax)}{sinh(bx)}$ could not be replaced by the exponent as before. As a result, the changes in temperature had a genuine effect on that fit.

Quantum Hall Regime

The first few filling factors in different graphs of R_{xy} vs B for different temperatures and voltage gates were extracted. The extracted values are quite close to integer values, fitting the theory. In addition to that, they are almost all even, fitting the spin degeneracy that disables odd filling factors. Only for $T = 1.7K$, where the Zeeman effect becomes more dominant, can the spin degeneracy be lifted and odd filling factors are extracted. Some filling factors are not as close to integral values as we would have wanted them to be. The somewhat inconsistent values could be the result of inaccurate measurement of the resistance by the lock-in amplifier. An additional cause may be impurities and other types of scattering events not accounted for which are amplified with increasing temperatures. Moving on to the two graphs of R_{xx} and R_{xy} VS V_g; it was established above that a change in the highest occupied Landau level occurs- for R_{xy} a plateau can be seen, and for R_{xx} there is a clear dip in the resistance (and at $T = 1.7K$ the Zeeman effect can also be noticed at the region of the dip in resistance). The reason why the highest occupied Landau level changes is because the Fermi level changes. As shown in previous sections, the charge carrier density becomes greater for higher voltage gates. The Fermi level also becomes higher when the charge carrier density becomes greater, leading it to eventually pass by a Landau level and cause the effect shown above.

References

[1] P. T. Coleridge. Small-angle scattering in two-dimensional electron gases. *Phys. Rev. B*, 44:3793–3801, Aug 1991.

[2] Peter Fulde and Klaus von Klitzing. *The Quantum Hall Effects Integral and Fractional*. Springer, 1995.

[3] W. J. Moore and R. T. Holm. Infrared dielectric constant of gallium arsenide. *Journal of Applied Physics*, 80(12):6939–6942, 1996.

[4] Edward M.Purcell and David J.Morin. *Electricity And Magnetism Third Edition*. Cambridge University Press, 2013.

[5] J.J. Sakurai and Jim Napolitano. *Modern Quantum Mechanics Second Edition*. Pearson, 2011.

[6] Steven H. Simon. *The Oxford Solid State Basics*. OXFORD University Press, 2013.

[7] M.Y. Simmons Tse-Ming Chen, C.T. Liang and D.A. Ritchie. Transport and quantum lifetime dependence on electron density in gated gaas/algaas heterostructures.

[8] Neil W.Ashcroft and N.David Mermin. *Solid State Physics*. Harcourt College Publishers, 1976.

[9] Claude Weisbuch and Borge Vinter. *Quantum Semiconductor Structures Fundamentals and Applications*. Academic Press,Inc, 1991.